Modelling excess properties of mineral and melt solutions over large P-T ranges: implications for phase relations and seismic velocities in the mantle

R. Myhill

Bayerisches Geoinstitut, Universität Bayreuth, Universitätsstrasse 30, 95447 Bayreuth, Germany

Abstract

Thermodynamic models of solid and liquid solutions in the Earth Sciences are increasingly used to calculate phase relations and seismic properties over large pressure and temperature ranges. Calculations often span over 1000 K and 5 GPa in studies of exhumation processes and metamorphism in subduction zones. Research into mantle phase relations and differentiation of the early Earth frequently involves calculations over 3000 K and 100 GPa. Despite spanning such huge ranges, a common approximation is that excess thermodynamic derivatives within solid solutions (entropy and volume) are pressure-temperature invariant. If these excesses are large, the approximation can result in large errors in gibbs free energy at high pressure and temperature, and errors in seismic velocities even within the range of calibration conditions.

In this paper, we present a solution to this problem by extending the subregular Margules mixing model using intermediate compounds to define the thermodynamic properties of solid solutions. Mathematical derivations are provided for excess properties (H^{ex}, S^{ex}, V^{ex}) and their pressure and temperature derivatives (K_T^{ex}, α^{ex}, Cp^{ex} etc.). We provide examples of pyroxene, garnet and melt solutions, showing that inclusion of a variable excess volume is vital to simulate observed phase relations and seismic velocities. Heuristics are sug-

*Corresponding author: R. Myhill
Email address: myhill.bob@gmail.com (R. Myhill)

gested for intermediate compounds where individual thermodynamic properties are poorly constrained.

Keywords: high pressure, excess properties

1. Introduction

Solution models are a vital part of estimating phase relations in the Earth. Typically, some functional form (often quadratic, cubic) is used to describe excess non-configurational energies between endmembers. Where necessary, the parameters describing the properties of the solid solution are allowed to vary as a function of pressure and temperature.

$$W_{ij} = W_{ij}^H + W_{ij}^V P + W_{ij}^S T \tag{1}$$

Models described in this way have been extremely successful in describing the properties of solid solutions up to pressures of a few GPa. Increasingly, such models are being used over larger and larger pressure ranges. For example, garnet models are now being used to estimate phase relations in the mantle transition zone, and models of metallic alloys and melts are being used to study the composition and evolution of the Earth's core. It is unlikely that large W^V and W^S terms will remain constant from low P-T to the conditions of interest. Another development is the increasing use of solution models to estimate seismic velocities in the mantle and core. Because seismic velocities are much more strongly dependent on the pressure gradient of the volume than the volume itself, traditional interaction terms of the form in Equation 1 are unlikely to produce satisfactory results. For these reasons, we introduce here a simple adaptation of mixing models, which use intermediate compounds to describe the excess properties of the solid solution as a function of pressure and temperature. With the added flexibility comes a large increase in the number of free parameters, so we also provide useful heuristics for the cases where individual parameters are unknown.

The new form of the model is illustrated with the use of three implementations for pyroxene, garnet and Fe-FeO melt. We show that for these cases:

a constant excess volume based on room pressure data is a bad approximation beyond a few GPa pressure, and major errors in seismic velocities and phase relations result from not incorporating reasonable decays in excess volume. The models in this study are all implemented in the open software *burnman*, a mineral physics toolkit written in python. The software, first described in Cottaar et al. (2014), was originally designed for seismic velocity calculations. It has since been augmented with thermodynamics functionality, including a range of different models for solid solutions.

2. The Extended Subregular Margules (ESM) model

The subregular Margules mixing model within a binary system approximates excess Gibbs free energies at any given pressure and temperature as a cubic function of composition (Helffrich and Wood, 1989):

$$\mathcal{G}^{xs} = W_{12}X_1X_2^2 + W_{21}X_1^2X_2 \tag{2}$$

In the ESM model, we define properties for each binary pair based on two intermediate compounds with compositions $X_i = X_j = 0.5$. For the special case of a symmetric mixing model, the properties for both intermediates are the properties of a compound with that composition; otherwise, both compounds are fictional. The interaction terms are now defined as:

$$W_{ij}^{\mathcal{G}} = 4(\mathcal{G}_{ij} + T\mathcal{S}_{ij}^{\mathrm{conf}}) - 2(\mathcal{G}_i + \mathcal{G}_j) \tag{3}$$

where $\mathcal{S}_{ij}^{\mathrm{conf}}$ is the configurational entropy of the intermediate compound, which depends on the number of sites on which mixing occurs. For a solution with n independent endmembers, and ignoring ternary terms, the excess nonconfigurational Gibbs free energy is (Helffrich and Wood, 1989)

$$\mathcal{G}^{xs} = \sum_{i=1}^{n}\sum_{j>1}^{n} X_iX_j \left(W_{ij}X_j + W_{ji}X_i + 0.5(W_{ij}+W_{ji}) \sum_{k}^{n} (1-\delta_{ik})(1-\delta_{jk})X_k \right) \tag{4}$$

Using this new model, we can now define the properties of the solid solution as follows:

$$\mathcal{G} = \sum_i X_i \mathcal{G}_i + \mathcal{G}^{xs} \tag{5}$$

$$\mathcal{H} = \sum_i X_i \mathcal{H}_i + \mathcal{H}^{xs} \tag{6}$$

$$\mathcal{S} = \sum_i X_i \mathcal{S}_i + \mathcal{S}^{xs} \tag{7}$$

$$\mathcal{V} = \sum_i X_i \mathcal{V}_i + \mathcal{V}^{xs} \tag{8}$$

$$C_P = \sum_i X_i C_P + T \left(\frac{\partial \mathcal{S}}{\partial T} \right)_P^{xs} \tag{9}$$

$$\alpha = \frac{1}{\mathcal{V}} \left(\sum_i X_i \alpha_i \mathcal{V}_i + \left(\frac{\partial \mathcal{V}}{\partial T} \right)_P^{xs} \right) \tag{10}$$

$$K_T = \frac{\mathcal{V}}{\sum_i \frac{X_i \mathcal{V}_i}{K_{Ti}} - \left(\frac{\partial \mathcal{V}}{\partial P} \right)_T^{xs}} \tag{11}$$

$$C_V = C_P - \mathcal{V} T \alpha^2 K_T \tag{12}$$

$$K_S = K_T \frac{C_P}{C_V} \tag{13}$$

$$\gamma = \frac{\alpha K_T \mathcal{V}}{C_V} \tag{14}$$

With the exception of the enthalpy excess, excess terms ($\mathcal{S}^{xs}$, $\mathcal{V}^{xs}$ etc) are derived in the same way as the excess Gibbs free energy (Equation 4), with interaction terms defined as follows:

$$W_{ij}^{\mathcal{S}} = 4(\mathcal{S}_{ij} - \mathcal{S}_{ij}^{\text{conf}}) - 2(\mathcal{S}_i + \mathcal{S}_j) \tag{15}$$

$$W_{ij}^{\mathcal{V}} = 4\mathcal{V}_{ij} - 2(\mathcal{V}_i + \mathcal{V}_j) \tag{16}$$

$$W_{ij}^{\partial \mathcal{V}/\partial P} = -4\mathcal{V}_{ij}/K_{Tij} + 2(\mathcal{V}_i/K_{Ti} + \mathcal{V}_j/K_{Tj}) \tag{17}$$

$$W_{ij}^{\partial \mathcal{V}/\partial T} = 4\alpha_{ij}\mathcal{V}_{ij} - 2(\alpha_i \mathcal{V}_i + \alpha_j \mathcal{V}_j) \tag{18}$$

$$W_{ij}^{\partial \mathcal{S}/\partial T} = \frac{4C_{Pij} - 2(C_{Pi} + C_{Pj})}{T} \tag{19}$$

Finally, excess enthalpy is defined as

$$\mathcal{H}^{xs} = \mathcal{G}^{xs} + T\mathcal{S}^{xs} \tag{20}$$

2.1. Heuristics

It is often the case that endmembers are particularly well studied, while the properties of the solid solution are constrained only by enthalpies of solution and volumes at room temperature and pressure. In the absence of other data, heuristics are required to constrain the properties of the intermediate compounds. In this study, we suggest that the following heuristics be used:

$$\mathcal{S}_{ij} = 0.5(\mathcal{S}_i + \mathcal{S}_j) + \mathcal{S}_{ij}^{\text{conf}} \tag{21}$$

$$C_{Pij} = 0.5(C_{Pi} + C_{Pj}) \tag{22}$$

$$\alpha_{ij} = 0.5\mathcal{V}\left(\frac{\alpha_i}{\mathcal{V}_i} + \frac{\alpha_j}{\mathcal{V}_j}\right) \tag{23}$$

$$K'_T = -\frac{\partial}{\partial P}\left(\mathcal{V}\left(\frac{\partial P}{\partial \mathcal{V}}\right)_T\right) \sim \mathcal{V}\left(\sum_i \frac{X_i\mathcal{V}_i}{K'_{Ti}+1}\right)^{-1} - 1 \tag{24}$$

If excess volumes are zero, the bulk modulus is given by Equation 11, with the differential term equal to zero. However, non-zero excess volumes are unlikely to remain constant with pressure and temperature. Mixing of elements with different ionic radii and chemical bonding on sites affects not only the packing efficiency, but also the mechanisms of compression. A positive excess volume implies a more open structure which will be more prone to volume decrease on compression.

We suggest that, in the absence of other data it should be assumed that $\left(\frac{\partial \mathcal{V}}{\partial P}\right)_T^{xs} \to 0$ as $P \to \infty$. Bulk moduli for intermediates can then be constrained.

$$K_T \sim 0.5(K_{Ti} + K_{Tj}) + \xi\left(\frac{K_{Ti}\mathcal{V}_j + K_{Tj}\mathcal{V}_j}{\mathcal{V}_i + \mathcal{V}_j} - 0.5(K_{Ti} + K_{Tj})\right) \tag{25}$$

The factor ξ before the second term on the RHS of Equation 25 modifies the rule of thumb proposed by Anderson and Anderson (1970) to estimate the compressibility of endmembers based on their molar volumes. Typically, a value of $\sim$6 provides a useful first estimate of ξ.

3. Examples

3.1. Pyroxene

Our first example is that of jadeite-aegirine pyroxene, an almost ideal solid solution (from a volumetric perspective). We use this model to illustrate that even when excess volumes are extremely small, excess bulk moduli are resolvable. The experimental data is that of Nestola et al. (2006), and the equation of state used is the Modified Tait (Holland and Powell, 2011). The fit to the volume data is shown in Figure 1.

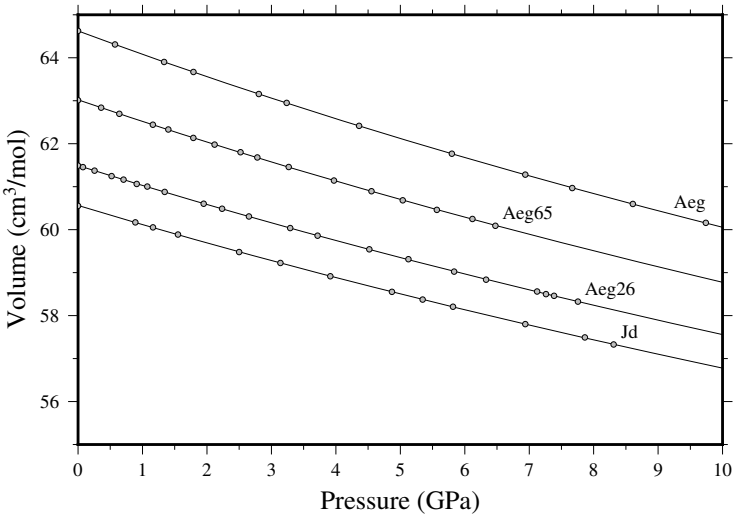

Figure 1: Pressure-volume data in the binary system Jadeite-Aegirine (Nestola et al., 2006), with the model proposed in this study.

Table 1: Jadeite-Aegirine mixing parameters to fit the room temperature data of Nestola et al. (2006). The K_0' for the intermediate compound is fixed to the value given by the heuristic proposed in the text. $K_0'' = -K_0'/K_0$.

	jadeite	aegirine	$jd_{50}ae_{50}$	$ae_{50}jd_{50}$
V_0 (cm^3/mol)	60.5640 ± 0.0001	64.6261 ± 0.0004	62.3641 ± 0.0005	62.4522 ± 0.0005
K_0 (GPa)	133.5 ± 0.2	116.0 ± 0.2	124.8 ± 0.5	126.7 ± 0.4
K_0'	4.6 [fixed]	4.4 [fixed]	4.4785 [heuristic]	4.4785 [fixed]

Using the derived properties of the solid solution, we can fit the excess volume as a function of pressure (Figure 2). The decay of excess volume as a function of pressure is in excellent agreement with the heuristic proposed in the previous section. The excess bulk modulus is ~ 10 times that of the $KV = c$ endmember rule of thumb (Anderson and Anderson, 1970).

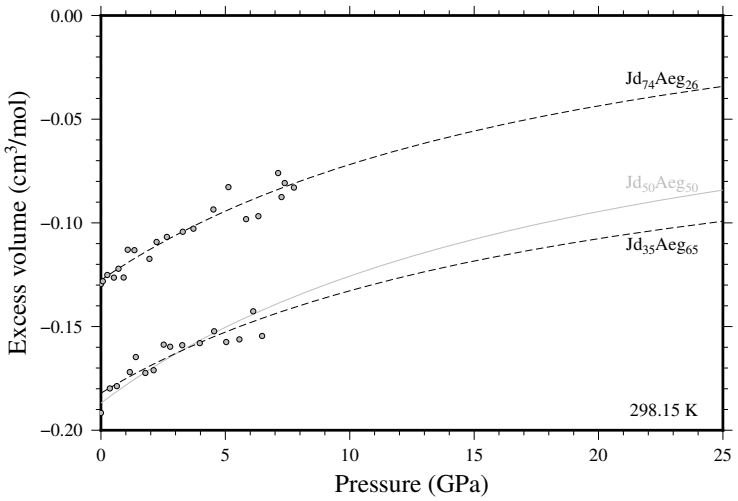

Figure 2: Excess volume for Jd-Aeg pyroxenes calculated from our model.

3.2. Garnet

Our second example is the pyrope-grossular join, which is well-known to have significant non-ideality and volumes of mixing (Newton et al., 1977; Bosenick and Geiger, 1997; Ganguly et al., 1996). Recently, it has been suggested that the excess volumes of mixing are ∼1 cm^3/mol, 2–3 times larger than previously suggested, and are associated with very large negative excess bulk moduli (Du et al., 2015). Here we compare the recent results with those predicted from a combination of the previous results and our heuristics. the excess volume of Du et al. (2015), approximating the solid solution as symmetric and using the heuristics described above. The data from Du et al. (2015) shows a clear 'w'-shaped pattern in bulk modulus, which the authors argue is the result of ordering around $Py_{50}Gr_{50}$. Since this pattern means that intermediate compositions will yield the smallest absolute excess bulk modulus, we fit the data from the $Py_{40}Gr_{60}$ sample and the $Py_{20}Gr_{80}$/$Py_{80}Gr_{20}$ samples separately (Table 2). The fit to the room temperature data is shown in Figure 3.

Table 2: Pyrope-Grossular mixing parameters to fit the P-V-T data of Du et al. (2015). The K_0' for the ordered intermediate compound is fixed to the value given by the heuristic proposed in the text. The extreme K_0 and K_0' for the disordered intermediate compound are required to avoid negative volume excesses at high pressure. $K_0'' = -aK_0'/K_0$, where $a = 1$ and $a = 52$ for the ordered and disordered compounds respectively.

	pyrope	grossular	$py_{50}gr_{50}$ (ord)	$py_{50}gr_{50}$ (disord)
V_0 (cm^3/mol)	113.14 ± 0.02	125.18 ± 0.03	120.13 ± 0.03	119.63 ± 0.06
K_0 (GPa)	168 ± 2	173 ± 2	159 ± 3	127 [see caption]
K_0'	4.4 [fixed]	5.5 [fixed]	4.975 [heuristic]	22 [see caption]
α_0 (10^{-5}/K)	2.58 ± 0.06	2.15 ± 0.05	2.12 ± 0.07	1.88 ± 0.16

If the excess volumes for the "ordered" fit apply to the py-gr join at high pressure and temperature, they correspond to differences in gibbs free energy of several kJ/mol, which will affect phase relations in the mantle transition zone and uppermost lower mantle. The negative excess bulk modulus will moderate this effect, and will also have a major effect on seismic velocities. P-wave, S-

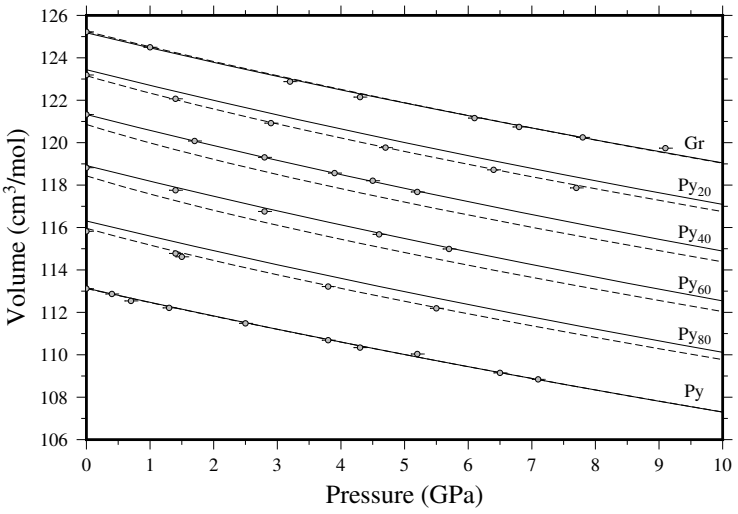

Figure 3: Pressure-volume data in the binary system Pyrope-Grossular (Du et al., 2015), with the models proposed in this study. The dotted lines are the fit to the data close to the center of the binary, while the dashed lines are the fit to the $Py_{20}Gr_{80}/Py_{80}Gr_{20}$ samples.

wave and bulk sound velocities are functions of isentropic bulk and shear moduli and density:

$$V_P = \sqrt{\frac{K_S + \frac{4}{3}G}{\rho}} \tag{26}$$

$$V_S = \sqrt{\frac{G}{\rho}} \tag{27}$$

$$V_\Phi = \sqrt{\frac{K_S}{\rho}} \tag{28}$$

We note that for natural garnet, $(\partial \ln V_S / \partial \ln V_P)_P \sim 1$ (Chai et al., 1997), and therefore $V_p/V_S \sim c$ with varying temperature. With this in mind, V_P and V_S should be constant fractions of the bulk sound velocity V_Φ.

To illustrate the effect of excess bulk moduli on seismic wave velocities, we plot V_Φ for a 50:50 molar mix of pyrope and grossular according to four solid solution models (Figure 4). The reduction of bulk sound velocities for the "ordered" endmember is $\sim$5%, comparable to the variation of seismic wavespeeds in the mantle at a given depth. Also noteworthy is the difference in pressure

dependence of the bulk sound velocities between the two models presented in this study. To avoid negative excess volumes in the "disordered" endmember, it was necessary to choose a very large K_0'. As a result, the excess volumes decay very rapidly, and the seismic wavespeeds at low pressures are extremely low. It is currently unclear what the volume behaviour of pyrope-grossular garnets is at high temperatures and pressures of 10–25 GPa, but the implication of our work is that using constant positive (or negative) excess volumes can significantly overestimate (underestimate) seismic velocities and/or underestimate (overestimate) the stability of intermediate compounds.

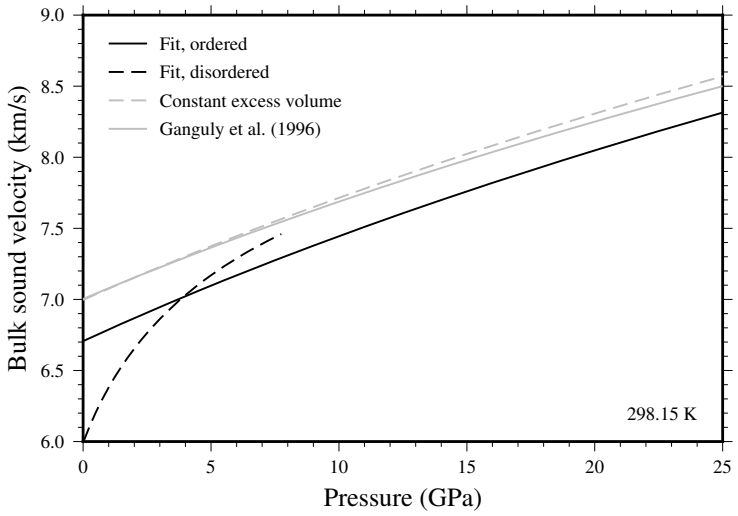

Figure 4: Bulk sound velocities of $Py_{50}Gr_{50}$ at room temperature according to the model of (Ganguly et al., 1996), a fixed excess volume based on room pressure data (Du et al., 2015) and the two full subregular models incorporating excess bulk moduli introduced in the present study.

3.3. Fe-FeO melt

Our final example is that of Fe-FeO melt. As oxygen may be one of the more abundant light elements in the core, understanding the thermodynamics of this liquid solution is an important part of understanding mantle-core differentiation and interaction over billions of years. At pressures <25 GPa, the Fe-FeO solution exhibits signficant non-ideality, with a large miscibility gap between ionic and metallic Fe-O liquids (Kowalski and Spencer, 1995; Tsuno et al., 2007; Frost et al., 2010). As pressure increases, this miscibility gap disappears, indicating a negative excess volume of mixing (Figure 5). To explain the increase in eutectic temperature with pressure, Komabayashi (2014) suggest that mixing becomes essentially ideal at >100 GPa.

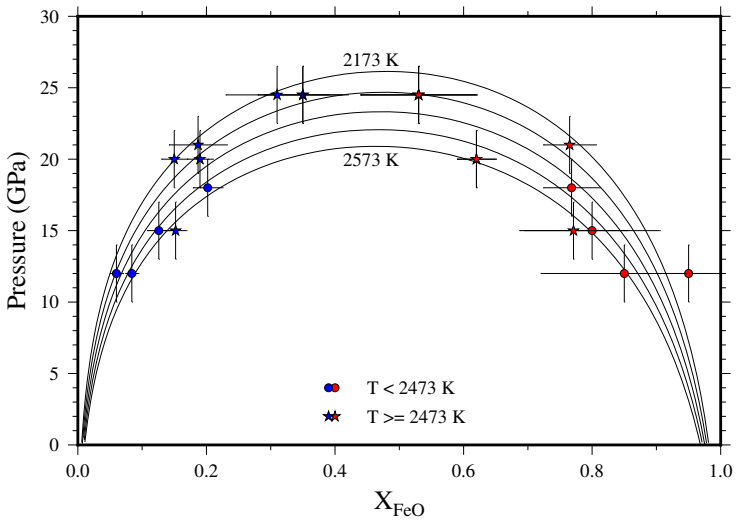

Figure 5: Fe-O solvus

To model processes of mantle differentiation and core formation, it would be extremely useful to have a single model describing the properties of melts over relevant pressure and temperature ranges. Clearly a high pressure ideal model cannot be reconciled with a low pressure model with large excess volumes of mixing without incorporating excess bulk moduli and thermal expansivities. Below ~25 GPa, the properties of the liquid can be estimated using the compositions

of coexisting metallic and ionic liquid (Tsuno et al., 2007; Frost et al., 2010). The chemical potentials of Fe and FeO are equal in the ionic and metallic liquids, providing the two constraints necessary to estimate Margules parameters at each pressure and temperature (Figure 6).

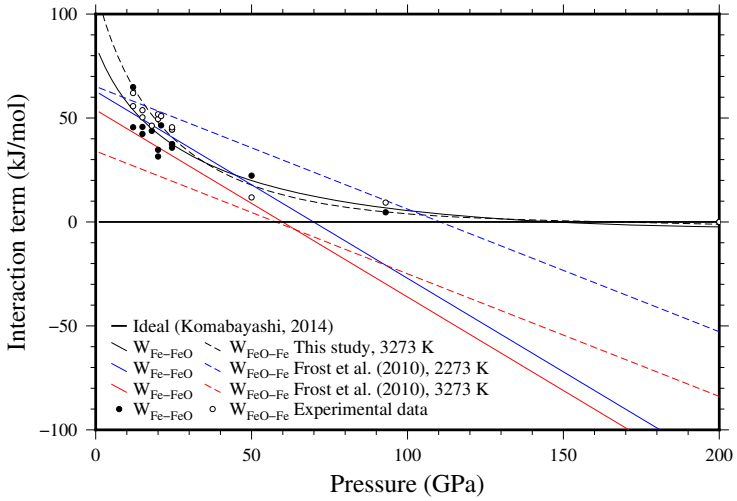

Figure 6: Interaction terms in Fe-FeO melt as a function of pressure.

At >25 GPa, the pressure, temperature and compositions of eutectic liquid at high pressure (Seagle et al., 2008) provide further constraints, providing we know the relative gibbs free energies of liquid and solid Fe and FeO. Here, we fit the thermodynamic properties of the FCC and HCP iron endmembers and of B1 FeO to published P-V-T data and phase boundaries. The liquid endmembers are fit with available room pressure data, and the effect of pressure is estimated using constraints on the melting curves from Anzellini et al. (2013), Seagle et al. (2008) and Ozawa et al. (2011). The uncertainties on composition and temperature of the eutectic are rather large, so these data are supplemented by the requirement that excess volumes become zero at very high pressure. The parameters used to create the fits in Figures 6 and 7 are given in Table 3. In this work, we fix excess entropy and thermal expansion to zero. The majority of the <25 GPa data was collected within a ∼200 K temperature range, and is associated with similar temperature uncertainties, which introduces very large uncertainties in

excess entropies. Add to that the possibility of phase separation during quench and the large uncertainty in coexisting ionic/metallic melt compositions, there is no clear evidence for the large temperature dependence proposed by Frost et al. (2010), although they do slightly improve the fit to the data (mostly by increasing the pressure at which the solvus closes at high temperature).

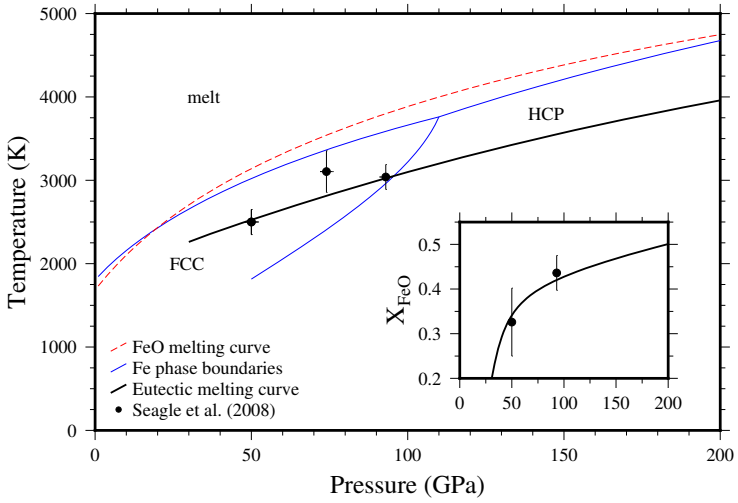

Figure 7: Melting temperature in the Fe-O system as a function of pressure. Inset: eutectic composition in the Fe-O system.

Table 3: Excess Fe-FeO mixing parameters to fit the data in Figures 6 and 7 at a reference temperature of 1809 K and pressure of 50 GPa.

Property	$Fe_{50}FeO_{50}$	$FeO_{50}Fe_{50}$
H^{xs} (J/mol)	5000 ± 400	4400 ± 400
S^{xs} (J/K/mol)	0 [fixed]	0 [fixed]
V^{xs} (cm^3/mol)	-0.117 ± 0.009	-0.136 ± 0.009
K^{xs} (GPa)	28 ± 5	45 ± 5
K'^{xs}	-0.07 ± 0.12	-0.37 ± 0.12
a^{xs}	0 [fixed]	0 [fixed]

4. Discussion

The use of intermediate compounds to describe excess properties is an extremely simple but powerful concept that lends a great deal of flexibility to models without necessarily increasing the number of parameters which need to be fit to the available experimental data.

(Fan et al., 2015; Huang and Chen, 2014)

The heuristics suggested here place constraints on seismic properties which are significantly more strict than typical uncertainties on bulk moduli derived from ultrasonic interferometry, Brillouin scattering or static compression. For example, along the pyrope-majorite join, excess volumes are small (0.1 cm^3/mol) (Heinemann et al., 1997). With the assumption that excess volumes decrease to zero with increasing pressure, the excess bulk modulus is constrained to be <1 GPa. In comparison, the range in bulk modulus estimates anywhere along the pyrope-majorite join is about 10 GPa (see, for example **?**).

It is envisaged that such models will be very useful in modelling silicate and metallic melts, where excess volumes are large at low pressure, and rapidly decrease at higher pressure. Even in the MgO-SiO_2 system, excess entropies and volumes are strongly dependent on temperature and pressure (de Koker et al., 2013).

Finally, we note that the equations derived here are all quite general, and therefore easily applicable to a wide range of different equations of state.

5. Acknowledgments

RM is funded by the Advanced ERC Grant awarded to the "ACCRETE" project.

References

Anderson, D.L., Anderson, O.L., 1970. Brief report: The bulk modulus-volume relationship for oxides. Journal of Geophysical Research 75, 3494–3500.

Anzellini, S., Dewaele, A., Mezouar, M., Loubeyre, P., Morard, G., 2013. Melting of Iron at Earth's Inner Core Boundary Based on Fast X-ray Diffraction. Science 340, 464–466.

Bosenick, A., Geiger, C.A., 1997. Powder x ray diffraction study of synthetic pyrope-grossular garnets between 20 and 295 k. Journal of Geophysical Research: Solid Earth 102, 22649–22657.

Chai, M., Brown, J.M., Slutsky, L.J., 1997. The elastic constants of a pyrope-grossular-almandine garnet to 20 Gpa. Geophysical Research Letters 24, 523–526.

Cottaar, S., Heister, T., Rose, I., Unterborn, C., 2014. BurnMan: A lower mantle mineral physics toolkit. Geochemistry, Geophysics, Geosystems 15, 1164–1179.

de Koker, N., Karki, B.B., Stixrude, L., 2013. Thermodynamics of the MgO-SiO_2 liquid system in Earth's lowermost mantle from first principles. Earth and Planetary Science Letters 361, 58–63.

Du, W., Clark, S.M., Walker, D., 2015. Thermo-compression of pyrope-grossular garnet solid solutions: Non-linear compositional dependence. American Mineralogist 100, 215–222.

Fan, D., Xu, J., Ma, M., Liu, J., Xie, H., 2015. Pvt equation of state of spessartinealmandine solid solution measured using a diamond anvil cell and in situ synchrotron x-ray diffraction. Physics and Chemistry of Minerals 42, 63–72.

Frost, D.J., Asahara, Y., Rubie, D.C., Miyajima, N., Dubrovinsky, L.S., Holzapfel, C., Ohtani, E., Miyahara, M., Sakai, T., 2010. Partitioning of

oxygen between the Earth's mantle and core. Journal of Geophysical Research (Solid Earth) 115, 2202.

Ganguly, J., Cheng, W., Tirone, M., 1996. Thermodynamics of aluminosilicate garnet solid solution: new experimental data, an optimized model, and thermometric applications. Contributions to Mineralogy and Petrology 126, 137–151.

Heinemann, S., Sharp, T.G., Seifert, F., Rubie, D.C., 1997. The cubic-tetragonal phase transition in the system majorite ($Mg_4Si_4O_{12}$) - pyrope ($Mg_3Al_2Si_3O_{12}$), and garnet symmetry in the Earth's transition zone. Physics and Chemistry of Minerals 24, 206–221.

Helffrich, G., Wood, B.J., 1989. Subregular model for multicomponent solutions. American Mineralogist 74, 1016–1022.

Holland, T.J.B., Powell, R., 2011. An improved and extended internally consistent thermodynamic dataset for phases of petrological interest, involving a new equation of state for solids. Journal of Metamorphic Geology 29, 333–383.

Huang, S., Chen, J., 2014. Equation of state of pyrope-almandine solid solution measured using a diamond anvil cell and in situ synchrotron X-ray diffraction. Physics of the Earth and Planetary Interiors 228, 88–91.

Komabayashi, T., 2014. Thermodynamics of melting relations in the system Fe-FeO at high pressure: Implications for oxygen in the Earth's core. Journal of Geophysical Research (Solid Earth) 119, 4164–4177.

Kowalski, M., Spencer, P., 1995. Thermodynamic reevaluation of the C-O, Fe-O and Ni-O systems: Remodelling of the liquid, BCC and FCC phases. Calphad 19, 229 – 243.

Nestola, F., Boffa Ballaran, T., Liebske, C., Bruno, M., Tribaudino, M., 2006. High-pressure behaviour along the jadeite $NaAlSi_2O_6$-aegirine $NaFeSi_2O_6$ solid solution up to 10 GPa. Physics and Chemistry of Minerals 33, 417–425.

Newton, R.C., Charlu, T.V., Kleppa, O.J., 1977. Thermochemistry of high pressure garnets and clinopyroxenes in the system CaO-MgO-Al_2O_3-SiO_2. Geochimica et Cosmochimica Acta 41, 369–377.

Ozawa, H., Takahashi, F., Hirose, K., Ohishi, Y., Hirao, N., 2011. Phase Transition of FeO and Stratification in Earth's Outer Core. Science 334, 792–.

Seagle, C.T., Heinz, D.L., Campbell, A.J., Prakapenka, V.B., Wanless, S.T., 2008. Melting and thermal expansion in the Fe-FeO system at high pressure. Earth and Planetary Science Letters 265, 655–665.

Tsuno, K., Ohtani, E., Terasaki, H., 2007. Immiscible two-liquid regions in the Fe O S system at high pressure: Implications for planetary cores. Physics of the Earth and Planetary Interiors 160, 75–85.